



Twenty classic signs in oral and maxillofacial radiology

Galal Omami¹

Received: 15 May 2018 / Accepted: 26 July 2018 / Published online: 10 October 2018
© Japanese Society for Oral and Maxillofacial Radiology and Springer Nature Singapore Pte Ltd. 2018

Abstract

Teachers of radiology often employ the use of classic signs to help learners identify the typical appearance of various pathologies. This article is a compendium of simply-described classic signs in oral and maxillofacial radiology, including their use in differential diagnoses.

Keywords Classic signs · Education · Oral radiology · Diagnostic imaging

Introduction

Over the years, radiologists have established many metaphorical imaging signs to attribute meaning to disease- or anatomy-specific imaging patterns encountered in the clinical setting. Oral and maxillofacial imaging is no exception. As a specialty that deals with uncommon lesions and complex anatomy, both students and practicing dental clinicians may benefit from this simplistic, pattern-based approach. This review describes a compendium of the classic signs in oral and maxillofacial radiology and discusses their use in differential diagnoses. Unless otherwise acknowledged, all images are courtesy of the author's personal collection.

Classic imaging patterns

“Soap bubble and honeycomb” appearances

The internal structure of solid/multicystic ameloblastoma is typically mixed, with the presence of bony septa creating multiple internal compartments, or loculations. This pattern reflects the presence of cystic formations within the tumor.

These cystic regions remodel the trapped bone into curved shapes, providing a “soap bubble” pattern (large radiolucent compartments of variable size) or a “honeycomb” pattern (numerous small compartments) (Fig. 1). Generally, the compartments are large in the posterior mandible and small in the anterior mandible [1]. The soap bubble pattern may also be observed in odontogenic keratocysts and giant cell granulomas [2] (Fig. 2). Odontogenic myxomas, however, sometimes display a small number of straight, thin septa, resembling strings in a tennis racket.

“Sunray” appearance

Osteosarcoma is the second most common primary malignant bone tumor, with multiple myeloma the first [3]. Osteosarcomas can stimulate the formation of thin, straight spicules of bone, giving a “sunray” or “hair-on-end” appearance (Fig. 3). This formation occurs when the periosteum is displaced, partially destroyed, and/or disorganized [4]. Chondrosarcomas, fibrosarcomas, and metastatic breast and prostate tumors may also exhibit bone production with a “sunray” appearance [5].

“Spiked root” appearance

Benign tumors tend to resorb adjacent root surfaces in a smooth fashion. When root resorption is associated with malignant disease; however, the resorption often occurs in smaller quantities, causing thinning of the root into a “spiked” shape [6] (Fig. 4). In the absence of generalized periodontitis, widening of the periodontal ligament space that involves one or several adjacent teeth (characteristically

Galal Omami: Diplomate, American Board of Oral and Maxillofacial Radiology.

✉ Galal Omami
Galal.Omami@uky.edu

¹ Department of Oral Health Practice, Division of Oral Medicine, Diagnosis and Radiology, University of Kentucky College of Dentistry, 800 Rose Street, Room MN-320, Lexington, KY 40536-0297, USA



Fig. 1 Ameloblastoma of the left mandibular body. Panoramic view of the lesion shows numerous small compartments (“honeycomb” pattern)



Fig. 2 Cherubism. Panoramic image shows bilateral, multilocular “soap bubble” lesions and significant jaw expansion. The internal structure is indistinguishable from a central giant cell granuloma (Courtesy Dr. Behrang Moghaddamzade, Tehran, Iran)

limited to one side of the root) could be an early sign of malignancy (Garrington’s sign) [7] (Fig. 4).

“Sharpened pencil” appearance

Approximately 50% of patients with rheumatoid disease have temporomandibular joint (TMJ) involvement [8]. Rheumatoid arthritis is characterized by synovial proliferation (pannus) and secondary erosive changes in the bone. Images of the TMJ often show progressive erosion at the attachment of the synovial lining of the anterior and posterior condylar surfaces, resulting in a small, pointed condyle in a large fossa (“sharpened pencil” appearance) (Fig. 5). Eventually, the entire condyle may be destroyed, with only the neck remaining as the articulating surface.

“Tram-track” appearance

Monckeberg’s medial vascular calcification (arteriosclerosis) is characterized by degeneration and subsequent deposition of calcium in the medial coating of the artery.

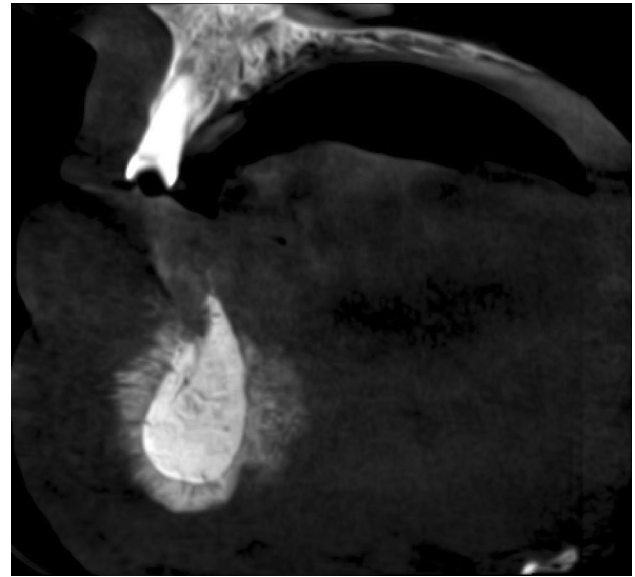


Fig. 3 Osteosarcoma of the mandible. Cross-sectional cone-beam computed tomography (CBCT) image shows an exuberant periosteal reaction with a “sunburst” pattern (Courtesy 3 Dimension Imaging, Allahabad, India)



Fig. 4 Osteosarcoma of the mandible. Note the increased bone density and irregular widening of the periodontal ligament spaces of the teeth of the left mandibular body (Garrington’s sign). Also, note the “spiking” resorption of the mesial root of the first molar

These deposits, however, do not narrow the vessel lumen or interfere with blood flow [9]. This type of calcification is most frequently seen in patients with diabetes mellitus or chronic renal failure [10]. Radiographically, the calcified vessel appears as a parallel pair of thin, radiopaque lines that outline the affected vessel. It is described as having a “tram-track” or “pipe stem” appearance (Fig. 6).

“Sausage-string” appearance

Sialodochitis is defined as inflammation of the ductal system of either the parotid or submandibular gland. It results in dilation of the involved duct secondary to distal

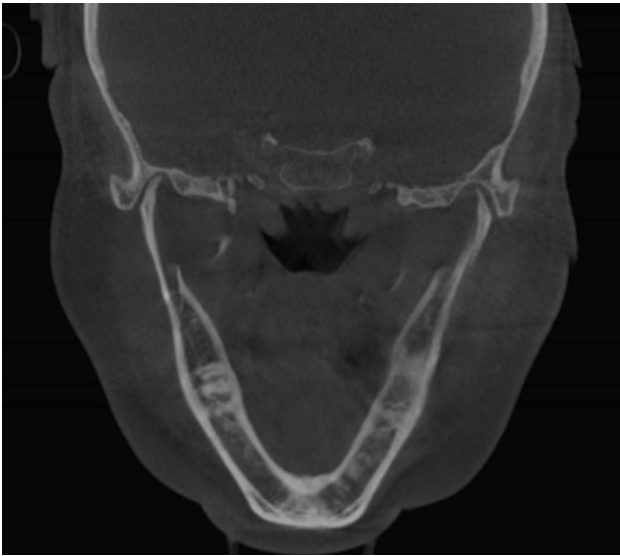


Fig. 5 Rheumatoid arthritis presented with temporomandibular joint (TMJ) pain and stiffness. Coronal CBCT image of the TMJ shows small remnants of the condylar heads after severe erosion, resulting in a “sharpened pencil” appearance of the condyle



Fig. 6 Sagittal CBCT image shows “tram-track” calcification of the facial artery (arrow)

obstruction. If interstitial fibrosis develops, however, it is seen on sialography as a “sausage-string” in the main and secondary ducts that is produced by intermittent strictures and dilations [11] (Fig. 7). More recently, these findings

have been seen with the use of magnetic resonance imaging [12].

“Hanging drop” appearance

The blowout orbital wall fracture results from a direct blow to the orbit. The force of the blow is transmitted to the orbital walls, among which the floor is most susceptible [13]. The classic “hanging drop” appearance of the herniated orbital content is clearly seen on a radiographic Waters’ view or on a coronal computed tomographic (CT) image, as is the “trapdoor” appearance of the displaced orbital floor. These signs are accompanied by an air–fluid level in the subjacent maxillary sinus (Fig. 8).

“Punched-out” appearance

A “punched-out” border is one that has a sharp boundary with no peripheral bone reaction. Its appearance is similar to that of a hole in a radiograph created with a paper punch. The border of the resulting hole is well-defined, and the surrounding bone has a normal appearance up to the edge of the hole. “Punched-out” lesions are typically indicative of multiple myeloma or Langerhans cell histiocytosis [14] (Fig. 9).

“Ground-glass” appearance

The radiological features of fibrous dysplasia vary considerably depending on the maturity of the lesion [15]. In the early stage, fibrous dysplasia appears as a unilocular or multilocular radiolucency with ill-defined or well-defined borders. In the middle stage, radiopaque tissue appears in the radiolucent structure. In the mature stage, the internal structure has a granular, radiopaque pattern

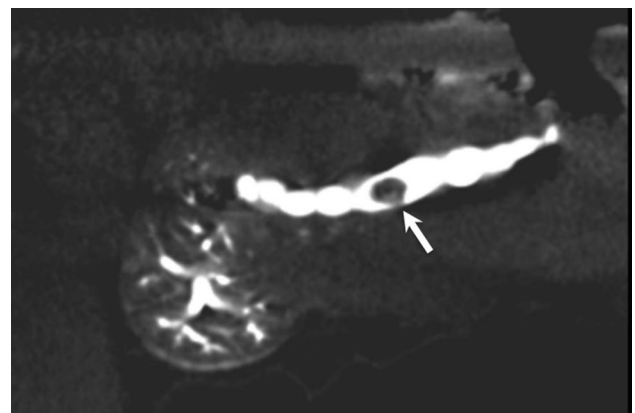


Fig. 7 CBCT sialogram of the submandibular gland shows a negative filling defect in the proximal portion of Wharton’s duct (arrow). The defect suggests a minimally calcified sialolith (mucus plug). The “sausage-string” appearance of the main duct is typical of sialodochitis



Fig. 8 Waters view shows the “hanging drop” sign of the orbital floor blowout fracture with herniation of soft tissue into the maxillary sinus (arrow). An air–fluid level is visible in the maxillary sinus (arrowhead)



Fig. 9 Langerhans cell histiocytosis. Lateral skull projection shows a well-defined, “punched-out” lesion in the parietal bone (arrow). In advanced cases, multiple lesions may enlarge and coalesce to form “maplike” areas referred to as “geographic skull”

often appearing as “ground-glass” opacities (resembling glass that has been ground or etched to create a roughened, nontransparent surface) with ill-defined borders blending into normal adjacent bone (Fig. 10). Bone changes associated with hyperparathyroidism may show a similar pattern on a diagnostic image.

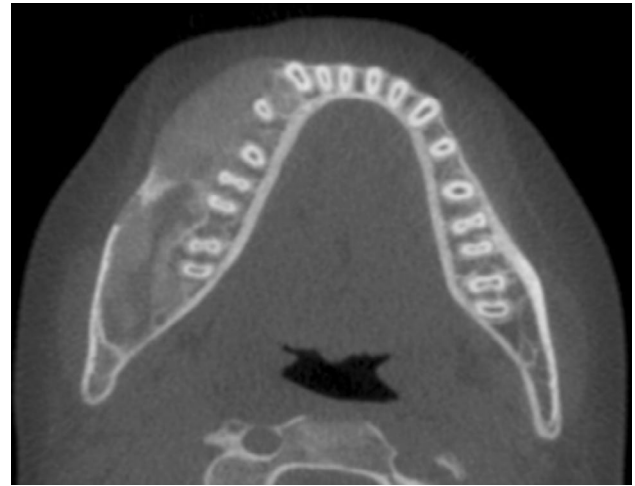


Fig. 10 Axial CBCT image of fibrous dysplasia shows an expansile lesion of the right mandible with the typical “ground-glass” appearance

“Cotton-wool” appearance

The late stage of Paget’s disease of bone classically presents with rounded, dense, radiopaque patches of abnormal bone, creating a “cotton-wool” appearance. Florid cemento-osseous dysplasia may also present with “cotton-wool”-type radiopaque regions (Fig. 11). However, these lesions are centered above the inferior alveolar nerve canal and most commonly have a radiolucent capsule, whereas in Paget’s disease the entire mandible may display hypercementosis [16].

“Moth-eaten” appearance

The first radiographic evidence of osteomyelitis is often a slight decrease in the density of the involved bone, with a loss of sharpness of the trabecular structure [17]. The bone resorption becomes more profound with time, resulting in ill-defined lytic areas throughout the affected bone. This pattern sometimes takes the form of “moth-eaten” bone (similar to a piece of clothing ruined by moth larvae) (Fig. 12). Early-to-moderate bone invasion by aggressive carcinoma often produces a permeative, or “moth-eaten,” pattern of bone destruction. Here, the overall bone density decreases, and the bone markings become indistinct.

“Floating teeth” appearance

When the jaws are affected by Langerhans cell histiocytosis, the change usually consists of focal alveolar bone loss resembling localized severe periodontitis [18] (Fig. 13). The alveolar lesions commonly start in the midroot region of the teeth, with bone destruction progressing in a circular

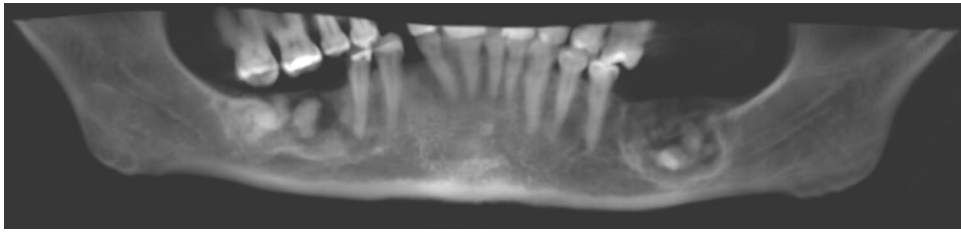


Fig. 11 Florid cemento-osseous dysplasia. CBCT-generated panoramic image shows multiple, bilateral, mixed radiopaque-radiolucent lesions in the mandible. The epicenter of all lesions is above the inferior alveolar canal. The internal radiopacity displays “cotton-wool” sclerotic

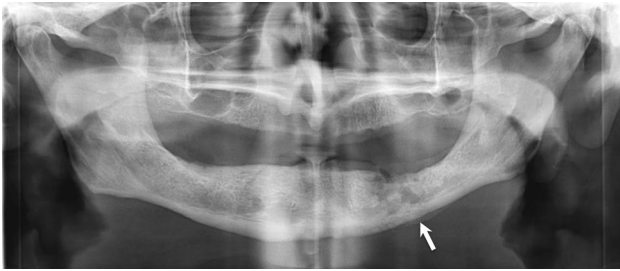


Fig. 12 Panoramic image shows the typical “moth-eaten” pattern of bone destruction, areas of rarefaction, sequestrum formation, and a periosteal reaction at the inferior border of the mandible (arrow)



Fig. 13 Panoramic radiograph of the right second molar teeth “floating in air” because of periodontitis. Note the reactive sclerosis surrounding the periodontal defect and the generalized marginal bone loss and calculus

manner to include a portion of the superior border of the alveolar process, giving the impression that a segment of the alveolar process has been scooped out. In some cases, destruction of the supporting alveolar bone is so severe that the teeth appear to be floating in air [19]. The periphery usually appears punched-out. However, the presence of reactive marginal sclerosis indicates periodontitis.

“Bull’s-eye” appearance

When the roots are dilacerated mesially or distally, the condition is clearly visible on a periapical film. However, when

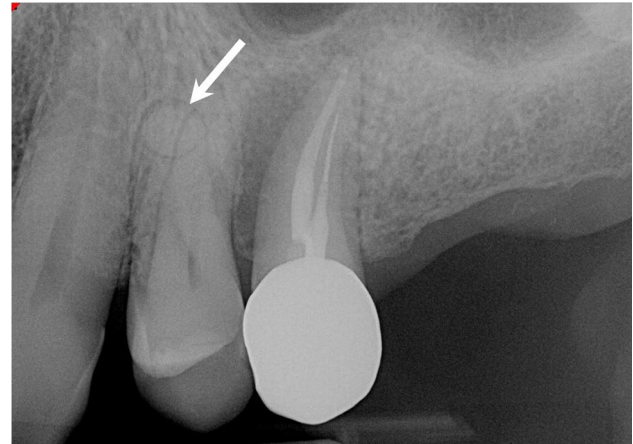


Fig. 14 Periapical radiograph of the maxillary premolars. The root tip of the first premolar root is dilacerated in the buccolingual direction so its long axis lies along the path of the X-ray beam. Note the “bull’s eye” appearance produced by the root canal, root tip, and periodontal ligamental space (arrow)

the roots are dilacerated facially or lingually, the central X-ray beam passes parallel to the long axis of the dilacerated portion of the root. This pattern, in turn, leads to a round, radiopaque area with a central dark spot (caused by the apical foramen of the root canal), giving the appearance of a “bull’s eye” (Fig. 14). The periodontal ligamental space around this dilacerated portion may appear as a radiolucent halo encircling the radiopaque area.

“Onion-skin” appearance

Salivary gland stones (sialoliths) are most common (80–90%) in the submandibular gland. Some of the reasons given for the higher incidence of sialolithiasis in the submandibular gland than in the parotid gland are the more viscous nature and higher mineral content of submandibular gland secretions and the more tortuous course and uphill flow of Wharton’s duct. Radiographically, sialoliths usually have a smooth shape. Their internal structure is most often homogeneously radiopaque with evidence of a laminated pattern, giving sialoliths an “onion-skin”

appearance (Fig. 15). Periosteal reaction consists of several parallel, concentric layers of periosteal new bone laid down between the periosteum and the outer cortex. This pattern is most commonly seen in inflammatory lesions (e.g., chronic osteomyelitis with proliferative periostitis) and rarely in tumors such as Ewing sarcoma and Langerhans cell histiocytosis [5].

“Cookie-bite” appearance

The term “cookie-bite” lesion was first used in the medical literature by Deutsch et al. to describe a saucerized, osteolytic, cortical, metastatic lesion derived from bronchogenic carcinoma [20]. Although “cookie-bite” metastasis can develop from other primary malignancies, the most common primary lesion is bronchogenic carcinoma [21] (Fig. 16). The “cookie-bite” appearance has also been observed in conjunction with osteomyelitis of the jaw [22].



Fig. 15 Mandibular occlusal image shows a calcified sialolith in Wharton's duct. Note the position and the hint at a laminated “onion-skin” internal pattern



Fig. 16 Panoramic image shows a “cookie-bite” pattern of bone destruction in the right mandible, a wide zone of transition with permeative changes within it, and lack of sclerosis at the margin

“Spoke-wheel” appearance

Central (intraosseous) hemangioma usually appears as a multilocular, expansile lesion that may be associated with displacement and resorption of adjacent teeth. When forming the basic multilocular pattern, however, the trabeculae may be arranged as a hub or in a spoke-of-a-wheel or honeycomb pattern [23]. Although the honeycomb appears to be nonspecific, the slightest hint of a “spoke-of-a-wheel” appearance is strongly suggestive of a central hemangioma (Fig. 17).

“Doughnut” appearance

Osteoma cutis is a rare soft tissue calcification in the skin. It is usually associated with chronic acne scars. Radiographically, osteoma cutis most commonly appears in the cheek as multiple, “doughnut”, or “washer-shaped”, radiopacities with radiolucent centers representing central marrow cavities [24] (Fig. 18).



Fig. 17 Hemangioma of the right mandible. Panoramic radiograph shows the lesion with coarse trabeculae radiating from a common center in a manner roughly resembling the spokes of a wheel. Dark spaces between trabeculae are blood cavities

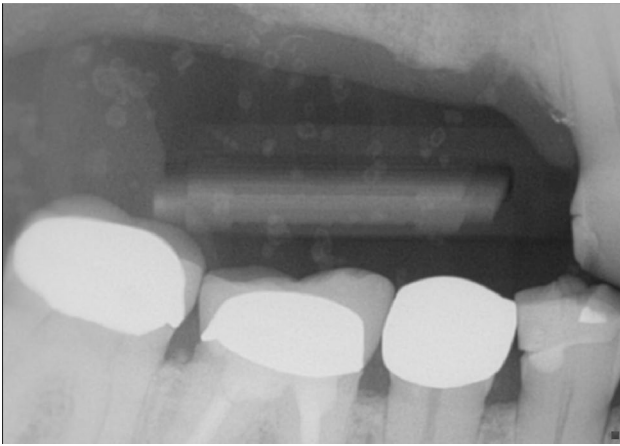


Fig. 18 Osteoma cutis. Bitewing image shows faint doughnut-shaped radiopacities in the cheek

“Beaten copper” appearance

The “beaten copper” appearance refers to prominent cranial markings seen on skull radiographs. These markings are thought to correspond to the gyral pattern of the growing brain and are generally considered a normal finding in children. A diffuse “beaten copper” appearance, however, has been shown to be related to elevated intracranial pressure from the growing brain in patients with premature craniosynostosis [25]. These markings may appear as multiple radiolucent areas that resemble hammered copper (Fig. 19).

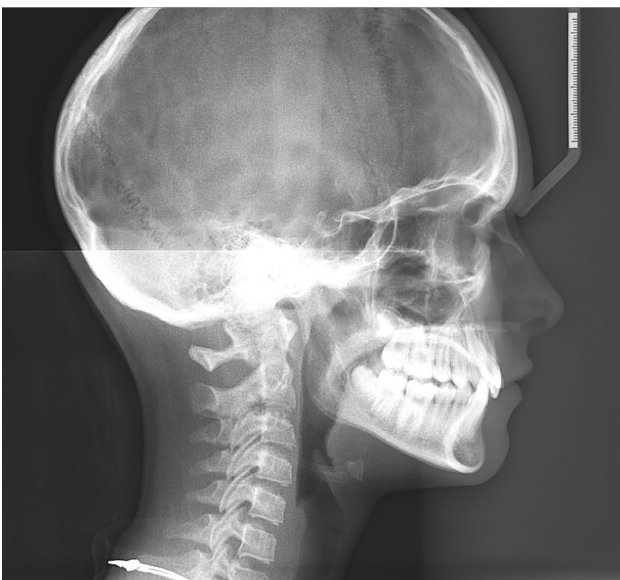


Fig. 19 Lateral cephalometric view shows convolitional markings (“beaten-copper” appearance) in a patient without a known history of craniosynostosis

“Bird’s beak” appearance

Degenerative joint disease, also known as osteoarthritis and osteoarthrosis, is a non-inflammatory disease characterized by the breakdown of the articular cartilage leading to eventual degeneration of the underlying bone. Degenerative joint disease is thought to occur when the ability of the joint to adapt to excessive forces, through remodeling, is exceeded. Degenerative changes of the joint include flattening and irregularities of the articular surfaces, osteophytosis (projections of bone formation at the periphery of the articulating surfaces), and subchondral degeneration. Flattening and osteophyte formation results in “beaking” at the anterior aspect of the condyle [26] (Fig. 20).

Conclusion

Radiology students as well as practicing dental clinicians may benefit from becoming familiar with the classic signs observed during oral and maxillofacial imaging. The author believes that using this simplified, pattern-based approach not only helps narrow the differential diagnosis, it may guide management by suggesting the appropriate use of additional imaging while avoiding unnecessary testing.



Fig. 20 Panoramic radiograph shows bilateral flattening osteophyte formation at the anterior aspect of the condyles giving a “bird’s beak” appearance

Compliance with ethical standards

Conflict of interest Galal Omami declares that he has no conflict of interest.

Research involving human and/or animal rights This article does not contain any studies with human or animal subjects performed by any of the authors.

References

- Kim SG, Jang HS. Ameloblastoma: a clinical, radiographic, and histopathologic analysis of 71 cases. *Oral Surg Oral Med Oral Pathol Oral Radiol Endod.* 2001;91:649–53.
- Kruse-Lösler B, Diallo R, Gaertner C, Mischke KL, Joos U, Kleinheinz J. Central giant cell granuloma of the jaws: a clinical, radiologic and histopathologic study of 26 cases. *Oral Surg Oral Med Oral Pathol Oral Radiol Endod.* 2006;101:346–54.
- Bennett JH, Thomas G, Evans AW, Speight PM. Osteosarcoma of the jaws: a 30-year retrospective review. *Oral Surg Oral Med Oral Pathol Oral Radiol Endod.* 2000;90:323–32.
- Wang S, Shi H, Yu Q. Osteosarcoma of the jaws: demographic and CT imaging features. *Dentomaxillofac Radiol.* 2012;41:37–42.
- Ida M, Tetsumura A, Kurabayashi T, Sasaki T. Periosteal new bone formation in the jaws: a computed tomographic study. *Dentomaxillofac Radiol.* 1997;26:169–76.
- Kawai N, Wakasa T, Asaumi J, Kishi K. A radiographic study on resorption of tooth root associated with malignant tumors. *Oral Radiol.* 2000;16:55–65.
- Garrington GE, Scofield HH, Cornyn J, Hooker SP. Osteosarcoma of the jaws: analysis of 56 cases. *Cancer.* 1967;20:377–91.
- Gynther GW, Tronje G, Holmlund AB. Radiographic changes in the temporomandibular joint in patients with generalized osteoarthritis and rheumatoid arthritis. *Oral Surg Oral Med Oral Pathol Oral Radiol Endod.* 1996;81:613–8.
- Lanzer P, Boehm M, Sorribas V, Thiriet M, Janzen J, Zeller T, et al. Medial vascular calcification revisited: review and perspectives. *Eur Heart J.* 2014;35:1515–25.
- Amann K. Media calcification and intima calcification are distinct entities in chronic kidney disease. *Clin J Am Soc Nephrol.* 2008;3:1599–605.
- Yousem DM, Kraut MA, Chalian AA. Major salivary gland imaging. *Radiographics.* 2000;216:19–29.
- Takagi Y, Sumi M, Van Cauteren M, Nakamura T. Fast and high-resolution MR sialography using a small surface coil. *J Magn Reson Imaging.* 2005;22:29–37.
- Lee HJ, Jilani M, Frohman L, Baker S. CT of orbital trauma. *Emerg Radiol.* 2004;10:168–72.
- Witt C, Borges AC, Klein K, Neumann HJ. Radiographic manifestations of multiple myeloma in the mandible: a retrospective study of 77 patients. *J Oral Maxillofac Surg.* 1997;55:450–3.
- Ricalde P, Magliocca KR, Lee JS. Craniofacial fibrous dysplasia. *Oral Maxillofac Surg Clin North Am.* 2012;24:427–41.
- White SC, Pharoah MJ. Other bone diseases. In: White SC, Pharoah MJ, editors. *Oral radiology: principles and interpretation.* 7th ed. St. Louis: Elsevier; 2013. pp. 402–25.
- Schuknecht B, Valavanis A. Osteomyelitis of the mandible. *Neuroimaging Clin N Am.* 2003;13:605–18.
- Kilborn TN, Teh J, Goodman TR. Paediatric manifestations of Langerhans cell histiocytosis: a review of the clinical and radiological findings. *Clin Radiol.* 2003;58:269–78.
- Dagenais M, Pharoah MJ, Sikorski PA. The radiographic characteristics of histiocytosis X: a study of 29 cases that involve the jaws. *Oral Surg Oral Med Oral Pathol Oral Radiol Endod.* 1992;74:230–6.
- Deutsch A, Resnick D. Eccentric cortical metastases to the skeleton from bronchogenic carcinoma. *Radiology.* 1980;137:49–52.
- Hendrix RW, Rogers LF, Davis TM Jr. Cortical bone metastases. *Radiology.* 1991;181:409–13.
- Omami G. “Cookie-bite” lesion of the mandible. *J Am Dent Assoc.* 2017;148:530–4.
- Zlotogorski A, Buchner A, Kaffe I, Schwartz-Arad D. Radiological features of central haemangioma of the jaws. *Dentomaxillofac Radiol.* 2005;34:292–6.
- Shigehara H, Honda Y, Kishi K, Sugimoto T. Radiographic and morphologic studies of multiple miliary osteomas of cadaver skin. *Oral Surg Oral Med Oral Pathol Oral Radiol Endod.* 1998;86:121–5.
- Tuite GF, Evanson J, Chong WK, Thompson DN, Harkness WF, Jones BM, et al. The beaten copper cranium: a correlation between intracranial pressure, cranial radiographs, and computed tomographic scans in children with craniosynostosis. *Neurosurgery.* 1996;39:691–9.
- Larheim TA, Abrahamsson AK, Kristensen M, Arvidsson LZ. Temporomandibular joint diagnostics using CBCT. *Dentomaxillofac Radiol.* 2015;44:20140235.